Paper presented at the International Symposium on High Energy Spin Physics and Polarization Phenomena in Nuclear Physics, Bloomington, Sept. 15–22

TRI-PP-94-96
Oct 1994

AB

Measurement of charge symmetry breaking in np elastic scattering at 350 MeV[1]

R. Abegg*, A.R. Berdoz†, J. Birchall†, J.R. Campbell†, C.A. Davis*†, P.P.J. Delheij*, L. Gan†, P.W. Green*‡, L.G. Greeniaus‡, D.C. Healey*, R. Helmer*, N. Kolb‡, E. Korkmaz‡, L. Lee†, C.D.P. Levy*, J. Li‡, C.A. Miller*, A.K. Opper‡, S.A. Page†, H. Postma§, W.D. Ramsay†, J. Soukup‡, G.M. Stinson*‡, W.T.H. van Oers†, A.N. Zelenski*, J. Zhao†

TRIUMF, 4004 Wesbrook Mall, Vancouver, B.C. Canada V6T 2A3
†University of Manitoba, Winnipeg, Manitoba, Canada R3T 2N2
‡University of Alberta, Edmonton, Alberta, Canada, T6G 2N5
§Technische Hogeschool, Delft, the Netherlands, 2600 GA

Abstract. TRIUMF Experiment 369, a measurement of charge symmetry breaking in np elastic scattering at 350 MeV, has completed data taking. Scattering asymmetries were measured with a polarized (unpolarized) neutron beam incident on an unpolarized (polarized) frozen spin target. Coincident scattered neutrons and recoil protons were detected by a mirror symmetric detection system in the center-of-mass angle range from 50° – 90°. A preliminary result for the difference of the zero-crossing angles, where analyzing powers cross zero, is $\Delta\theta_{cm} = 0.445° \pm 0.054°(\text{stat.}) \pm 0.051°(\text{syst.})$ based on fits over the angle range $53.4° \leq \theta_{cm} \leq 86.9°$. The difference of the analyzing powers $\Delta A \equiv A_n - A_p$, where the subscripts denote polarized nucleons, was deduced with $dA/d\theta_{cm} = (-1.35 \pm 0.05) \times 10^{-2}\text{deg}^{-1}$ to be $[60 \pm 7(\text{stat.}) \pm 7(\text{syst.}) \pm 2(\text{syst.})] \times 10^{-4}$.

INTRODUCTION

The study of isospin symmetry breaking is of fundamental interest since it relates to the mass difference of the quarks of the first generation, the up and down quarks with $m_d - m_u > 0$, in addition to the well-understood electromagnetic interaction(1). Early evidence for charge independence breaking and charge symmetry breaking (CSB) came from the differences in the nucleon-nucleon $^1S_0$ scattering lengths(2) and from the binding energy differences of mirror nuclei(3). The latter is the well-known Okamoto-Nolen-Schiffer anomaly. Theoretical interpretations of these observations carry uncertainties due to the subtraction of electromagnetic interaction effects. CSB in the np system belongs to a different class of charge symmetry breaking. It has the advantage of the absence of the Coulomb interaction.

Charge symmetry in the np system leads to the complete separation of the isoscalar and isovector components of the np interaction. This in turn leads to the equality of the differential cross sections for polarized neutrons scattering from unpolarized protons and vice versa. As a result, $A_n(\theta) \equiv A_p(\theta)$ where A denotes the analyzing power and the subscript represents the polarized nucleon. A nonvanishing asymmetry difference is directly proportional to the isospin triplet-singlet, spin singlet-triplet mixing amplitudes and therefore direct evidence of a charge-asymmetric interaction, anti-symmetric under the interchange of the two nucleons in isotopic spin space.

The scattering matrix for np elastic scattering can be expressed in terms of the formalism of LaFrance and Winternitz(4) as

$$M(\vec{k}_f, \vec{k}_i) = \frac{1}{2}\Big\{(a+b) + (a-b)(\vec{\sigma}_1 \cdot \hat{n})(\vec{\sigma}_2 \cdot \hat{n}) + (c+d)(\vec{\sigma}_1 \cdot \hat{m})(\vec{\sigma}_2 \cdot \hat{m}) + (c-d)(\vec{\sigma}_1 \cdot \hat{\ell})(\vec{\sigma}_2 \cdot \hat{\ell}) + e(\vec{\sigma}_1 + \vec{\sigma}_2) \cdot \hat{n} + f(\vec{\sigma}_1 - \vec{\sigma}_2) \cdot \hat{n}\Big\}. \quad (1)$$

Here, $\hat{\ell}, \hat{m}$ and $\hat{n}$ are unit vectors given as

$$\hat{\ell} = \frac{\vec{k}_i + \vec{k}_f}{|\vec{k}_i + \vec{k}_f|}; \quad \hat{m} = \frac{\vec{k}_f - \vec{k}_i}{|\vec{k}_f - \vec{k}_i|}; \quad \hat{n} = \frac{\vec{k}_i \times \vec{k}_f}{|\vec{k}_i \times \vec{k}_f|}; \quad (2)$$

with $\vec{k}_i$ and $\vec{k}_f$ the initial and final state center-of-mass nucleon momenta. The amplitudes a, b, c, d, e, and f are functions of center-of-mass energy E and scattering angle θ, with f the isotopic spin mixing amplitude. Written explicitly, the difference in the analyzing powers

$$\Delta A(\theta) \equiv A_n(\theta) - A_p(\theta) = \frac{2}{\sigma_0} \mathcal{R}e(b^* f), \quad (3)$$

is proportional to f. The quantity σ_0 is the differential cross section for the scattering of unpolarized neutrons from unpolarized protons.

The first measurement of charge symmetry breaking in np elastic scattering was performed at TRIUMF(5). The measurement of $\Delta A \equiv A_n - A_p$, at the zero-crossing angle of the average analyzing power, at an incident neutron energy of 477 MeV, yielded $\Delta A = (47 \pm 22 \pm 8) \times 10^{-4}$, an effect just over two standard deviations. More recently the results of a similar experiment at a neutron energy of 183 MeV performed at IUCF have been

[1]Work supported in part by the Natural Sciences and Engineering Research Council of Canada.

reported(6). The measured value of $\Delta A \equiv A_n - A_p$, averaged over the angular range $82.2° \leq \theta_{cm} \leq 116.1°$ over which $< A(\theta) >$ averages to zero, is $(34.8 \pm 6.2 \pm 4.1) \times 10^{-4}$, where as above the first error represents mainly the statistical uncertainty and the second error the systematic uncertainty. The IUCF result differs from zero by 4.5 standard deviations. It differs from the value expected from the electromagnetic spin-orbit interaction by 3.4 standard deviations. This difference represented the most unambiguous experimental evidence of charge symmetry breaking in the nuclear interaction.

Extracting an angular distribution of $\Delta A(\theta)$ is more difficult. This follows directly from the expression for the difference in the asymmetries for beam and target polarized, respectively, or

$$\epsilon_b(\theta) - \epsilon_t(\theta) = \Delta A(\theta)(P_b + P_t)/2 + < A(\theta) > (P_b - P_t)\,, \qquad (4)$$

pointing to the need for calibration of the beam and target polarizations (P_b and P_t) with an accuracy unattainable at present. In the analysis of the IUCF experiment this difficulty was overcome by adjusting the ratio of (P_b/P_t) applying a minimal variance procedure to $\Delta A(\theta)$ over the angular range of the experiment(6). Following this procedure a twelve point angular distribution was obtained. The procedure does not work at 477 MeV where $\Delta A(\theta)$ and $< A(\theta) >$ have zero-crossing angles in close proximity and consequently the angular dependencies are no longer orthogonal. If the theoretical calculations were precise in their predictions of the zero-crossing angle of $\Delta A(\theta)$, one could in principle also determine $\Delta P/ < P >$ with $\Delta P = P_b - P_t$ and $< P >$ $= (P_b + P_t)/2$, and consequently the angular distribution of $\Delta A(\theta)$ would follow.

The measured analyzing power differences of the IUCF and TRIUMF experiments are well-reproduced by theoretical predictions based on meson exchange potential models, which indirectly incorporate quark level effects(7). The calculations include contributions from one photon exchange (the magnetic moment of the neutron interacting with the current of the proton), from the neutron-proton mass difference affecting charged one π and ρ exchanges, and from the more interesting isospin mixing $\rho^0 - \omega$ meson exchange. Some other smaller effects (like 2π–exchange not included in ρ–exchange) have also been evaluated(8). The effects of $\pi\gamma$ exchanges have not yet been calculated. The effects of inelasticity amount to about 10% at 800 MeV but are vanishingly small at lower energies(9).

EXPERIMENT

A new experiment at 350 MeV has been performed at TRIUMF in order to delineate the various contributions to CSB. The experiment is similar in most aspects to the earlier TRIUMF measurement at 477 MeV. Designed as a null measurement, the difference of the zero-crossing angles where the analyzing powers A_n and A_p cross zero, respectively, is determined. With the slope, $dA/d\theta$, from phase shift analyses, or determined experimentally, the difference of the analyzing powers is obtained. Figure 1 illustrates the method to determine ΔA from the measured difference of the zero-crossing angles.

A 350 MeV neutron beam was produced using the (p,n) reaction on deuterium. The proton beam, polarized up to 80% and normal to the scattering plane, was obtained from an optically-pumped polarized ion source and accelerated by the cyclotron to 369 MeV, with polarizations up to 78%. The proton beam had an intensity of about 2 μA and was incident on a 0.217 ± 0.004 m long liquid deuterium (LD_2) target. Figure 2 shows a schematic layout of the beam line and experimental set-up. The polarization, the energy, the position and direction of the proton beam were monitored throughout the experiment and controlled (in the case of position and direction) using a feedback system coupling two sets of split-plate secondary electron emission monitors (which determined the median of the intensity distribution) with steering magnets upstream in the beam transport line. At the two sets of split-plate secondary emission monitors (SEMs), the beam position was kept fixed with a standard deviation of ± 0.05 mm in both x and y intensity profiles. The proton beam polarization was measured by two polarimeters. The beam energy monitor, based on range determinations, allowed the beam energy to be kept constant with a standard deviation of less than 36 keV (through minute changes in rf of the cyclotron and stripper foil position).

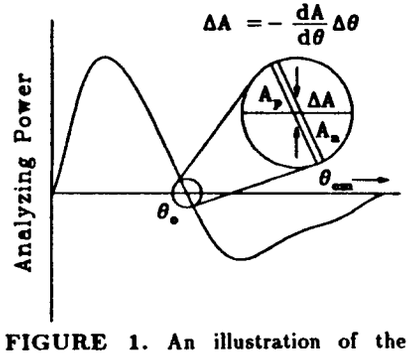

FIGURE 1. An illustration of the method employed to extract ΔA from the difference of the A_n and A_p zero-crossing angles for np elastic scattering. $dA/d\theta$ and $\Delta\theta_0$ are determined in the experiment.

The polarization was transferred from the proton to the neutron by making use of the large sideways to sideways polarization transfer coefficient $r_t(-0.88$ for $d(\vec{p},\vec{n})2p$ at 364 MeV). The proton beam polarization was rotated into the horizontal plane by a superconducting solenoid magnet. The neutrons passed a 3.3 m long, tapered steel collimator placed at 9° before impinging on a frozen spin type polarized proton target (containing butanol beads) positioned at 12.85 m from the center of the LD_2 target. The neutron beam polarization was rotated to the longitudinal direction and then to the normal direction by

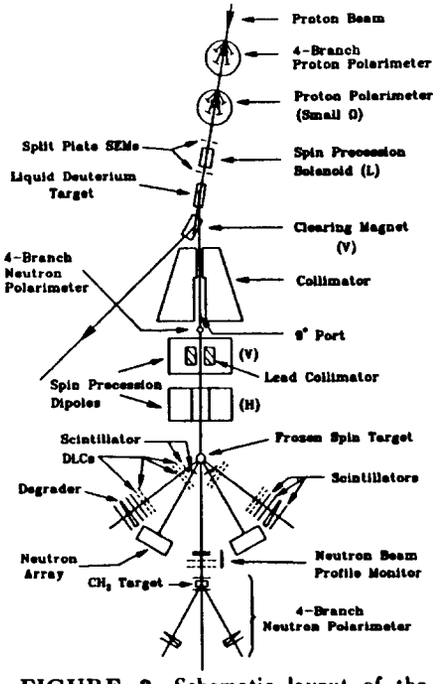

FIGURE 2. Schematic layout of the beam line and experimental setup.

a combination of two dipole magnets. The neutron beam polarization was monitored by two polarimeters, one at the exit of the collimator and the other 3.6 m downstream of the frozen spin target. The frozen spin target (FST) had typical polarizations of 80 to 90%. After being polarized, the spin of the "free" protons in the butanol beads was held "frozen" with a reduced, normal direction holding field of 0.22 T at a temperature of about 55 mK. For further details see Ref. (10).

The scattered neutrons were detected by scintillation detector arrays, each consisting of two banks of scintillator bars, one behind the other, with seven horizontally-stacked bars in each bank. Two additional bars with the same dimensions were placed vertically on each side beside the main arrays to enlarge the detection angle coverage. The recoil protons were detected by time-of- flight (TOF)/range telescopes, each consisting of a TOF start counter, four delay line wire chambers (DLCs), two scintillation counters, a wedge-shaped brass absorber and a veto scintillator. Only high energy protons from background processes can penetrate the absorber and trigger the veto counter. These events were rejected off-line by software. Figure 3 shows a detailed view of the detection system. To study the background (mainly due to quasi-elastic (n, np) scattering off the carbon of the butanol beads and other surrounding materials), the butanol beads were replaced by carbon beads having an equivalent target thickness with the rest of the target unchanged.

DATA ANALYSIS

The procedure of the data analysis was as follows: i) in order to identify possible sources of systematic errors, a study was made on a run-by-run basis of all system parameters recorded during data taking: beam energy, proton

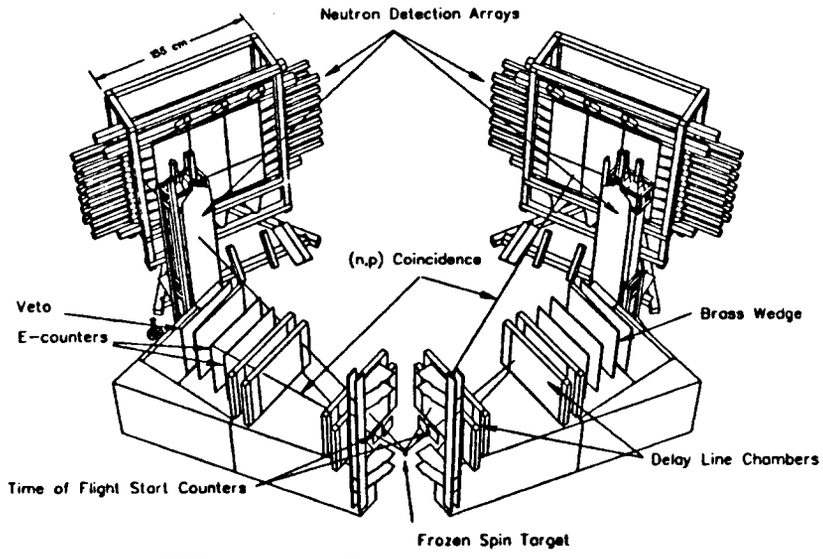

FIGURE 3. Detailed view of the detector system.

and neutron polarizations, SEM asymmetries, neutron profile, holding field strength and FST parameters; ii) elastic scattering np events were selected; iii) the asymmetry angular distributions and the zero-crossing angles were determined; and iv) corrections were made for contributions from quasi-elastic (n, np) background and for the effective average neutron beam energy difference of the polarized and unpolarized beam reflecting the energy-polarization correlation.

To select elastic scattering np events, proton and neutron tracks were reconstructed and their kinetic energies were calculated from their TOFs. Proton tracks were reconstructed from the information in the DLCs. At least one pair of coordinates (x and y) from each pair of DLCs (front and rear) was required. A loose cut of 40 mm on the total residuals of the proton tracks was applied to remove apparent multiple hits (about 3% of the total data). The proton energy was calculated from the TOFs between the TOF start counter and both scintillation counters. Event-by-event corrections were applied to the reconstructed proton angle and the proton energy to account for the proton deflection in the FST holding field, multiple scattering, and energy loss in the FST and detectors. The corrections were obtained from a Monte Carlo simulation of these processes. Neutron tracks were determined by their impact points in the neutron detector scintillator and the presumed

scattering points in the FST. The hit position of a neutron at the scintillator and its arrival time were determined by the difference and the average, respectively, of the timing signals recorded on both ends of each bar. The neutron origin in the FST was assumed to be along the central normal axis (y), and y_{no} was determined by the proton track reconstruction. The neutron energy was calculated from its TOF. The software energy threshold of the bars was varied by applying various cuts on the ADCs after gain matching and pedestal subtraction. Four kinematic variables: opening angle, coplanarity angle, energy sum and horizontal momentum balance were used to test for np events. The momentum-dependent sigmas of these variables were obtained from their distributions and the chi-squares (χ_i^2) were calculated for each event. Various chi-square tests including the individual $\chi_i^2 \leq 6$, 7.5, 9 or the four variable combined $\chi^2_{sum} \leq 10$, 15, 20 were applied to the data (Figs. 4a - 4e). Roughly 25% of the total data passed these cuts. The selected events were dominated by elastic scattering np events with a small contribution from the background.

Asymmetries were calculated based on the proton angle (θ_p) distributions (Fig. 4f). An "overlap" method(5) was used to obtain the asymmetries $\epsilon = \frac{r-1}{r+1}$, where $r = \sqrt{\frac{L+R-}{L-R+}}$ and zero-crossing angles (θ_0) were deduced from fits of the asymmetry angular distributions. To calculate ΔA from the measured $\Delta\theta_0, dA/d\theta$ is required. Because the $dA/d\theta$ from phase shift analyses show large discrepancies among different phase shift analyses and the FST polarization is known to about 2.5%(11), the experimentally determined $dA/d\theta$ is considered superior to the one from phase shift analyses.

The incident neutron beam energy was measured in two ways: the first was from the TOF between the cyclotron rf phase stabilized timing signal at the LD_2 target and the timing signal from the proton TOF start counter, the second was from the sum of the neutron and proton kinetic energies. To correct for the different effective average energy of the polarized and unpolarized neutron beam due to the energy dependence of the neutron polarization, Monte Carlo simulations were made (Figs. 5a - 5b). Comparisons with the experimental distributions were made after folding in the experimental resolution (taken to be a Gaussian). Good agreement was achieved as shown in Fig. 5c. The difference between the average effective neutron beam energy for polarized and unpolarized beams is calculated, based on these distributions, to be 0.4 MeV. A $d\theta_0/dE$ = -0.055°/MeV deduced from phase shift analyses was used resulting in a correction of +0.022° (cm) for the zero-crossing angle of A_n.

Background data obtained with carbon beads replacing the butanol beads were analyzed in an identical fashion. To remove some hydrogen contamina-

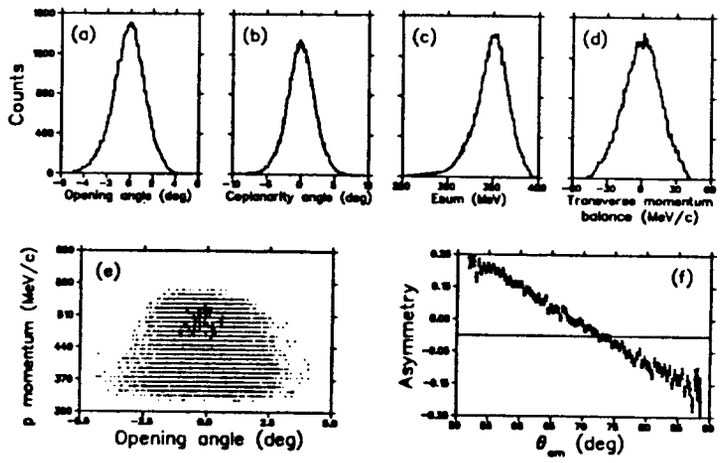

FIGURE 4. (a - d) kinematic variable distributions after $\chi_i^2 \leq 6$ cuts; (e) proton momentum versus opening angle distribution to determine the momentum dependence of the sigmas; (f) asymmetry distribution as function of the center-of-mass scattering angle.

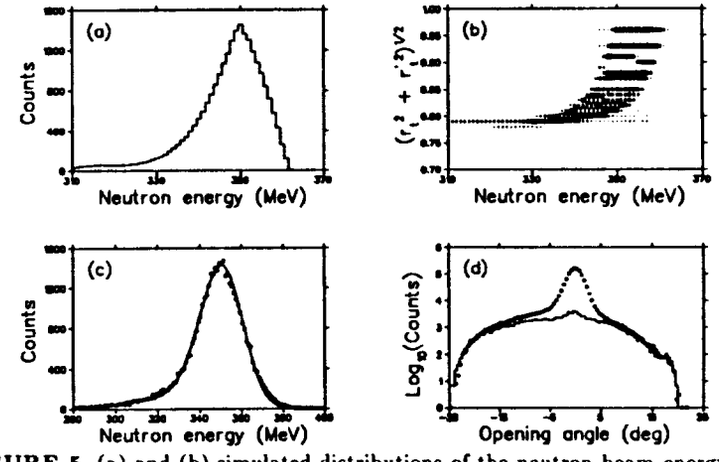

FIGURE 5. (a) and (b) simulated distributions of the neutron beam energy and neutron energy versus effective r_t for the reaction $D_2(\vec{p},\vec{n})2p$; (c) comparison of the simulated and experimental measured neutron beam energy after applying a Gaussian distribution to the curve in (a) reflecting the experimental resolution; (d) opening angle distribution for the butanol target data, shown as the upper curve; the lower curve is obtained from the carbon target data. The carbon target data have been normalized to the butanol data by matching the tails of the distributions.

tion due to a hydrogen-containing resistor of the FST and super-insulation material around the target cell, various methods were used including applying additional cuts of $\chi_t^2 \geq 1$ or subtracting the hydrogen peak with normalized butanol target data. It was determined that 4% of the events which passed the $\chi_t^2 \leq 7.5$ cuts were from the background (Fig. 5d) and that the analyzing power of the background is $A_b = -0.004 \pm 0.007$. A correction of $\Delta A = (+1.6 \pm 2.8) \times 10^{-4}$ for background contribution was applied to the result based on this evaluation.

PRELIMINARY RESULT AND DISCUSSION

A preliminary result of the data analysis shows the difference of the zero-crossing angles to be $\Delta\theta_{cm} = 0.445° \pm 0.054°(\text{stat.}) \pm 0.051°(\text{syst.})$ based on fits over the angle range $53.4° \leq \theta_{cm} \leq 86.9°$. With $dA/d\theta_{cm} = (-1.35 \pm 0.05) \times 10^{-2}$ deg^{-1}, as determined from the measured asymmetries with the target polarized, the value of $\Delta A \equiv A_n - A_p$, is $[60 \pm 7(\text{stat.}) \pm 7(\text{syst.}) \pm 2(\text{syst.})] \times 10^{-4}$. The second systematic error reflects the uncertainty in $dA/d\theta_{cm}$.

The triptych in Fig. 6 shows the experimental results for $\Delta A \equiv A_n - A_p$ for np elastic scattering, at 183 MeV(6), at 350 MeV, and at 477 MeV(5). The horizontal lines present the theoretical predictions of Iqbal and Niskanen (IN)

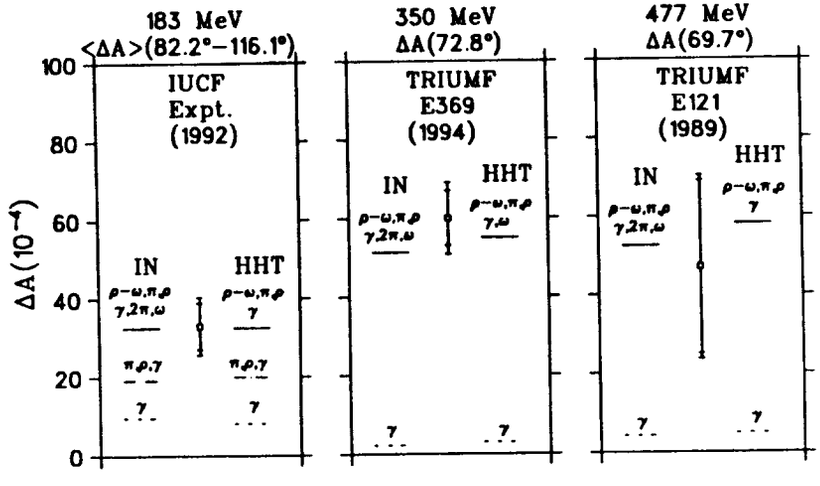

FIGURE 6. Experimental results for $\Delta A \equiv A_n - A_p$ for np elastic scattering at 183 MeV, 350 MeV and 477 MeV. The horizontal lines represent theoretical predictions of Iqbal and Niskanen (IN) and Holzenkamp, Holinde and Thomas (HHT).

and Holzenkamp, Holinde and Thomas (HHT). Note that the contributions corresponding to one photon exchange and to the np mass difference affecting charged π and ρ exchanges together suffice to give a theoretical prediction in agreement with the 350 MeV and 477 MeV TRIUMF results. This is because at these energies the angular distribution of the contributions due to $\rho^0 - \omega$ meson mixing crosses zero close to the zero-crossing angle of $< A(\theta) >$. The contribution due to 2π exchanges is small at all three energies. Reproducing the 183 MeV result from IUCF with the present calculations requires inclusion of the $\rho^0 - \omega$ meson mixing contribution, an approximately two standard deviation effect. Excluding the $\rho^0 - \omega$ meson mixing contribution will change the theoretical angular distributions of $\Delta A(\theta) \equiv A_n(\theta) - A_p(\theta)$ at 350 MeV and 477 MeV. A great deal of controversy has arisen regarding the role of $\rho^0 - \omega$ meson mixing in CSB(1). Consequently it is most important to extract any information regarding the angular distribution that can be obtained from the experimental data. More extensive data analysis is in progress and a more definitive systematic error for the 350 MeV data will be deduced.

REFERENCES

1. Miller, G.A., Nefkens, B.M.K. and Slaus, I., Phys. Rep. **194**, 1 (1990); Miller, G.A. and van Oers, W.T.H., in "Symmetries and Fundamental Interactions in Nuclei," ed. Haxton, W.C. and Henley, E.M. (World Scientific Publishing Co., Singapore), in press; and references therein.
2. Dumbrajs, O., *et al.*, Nucl. Phys. B **216**, 277 (1983).
3. Nolen, Jr., J.A. and Schiffer, J.P., Ann. Rev. Nucl. Sci. **19**, 471 (1969).
4. LaFrance, P. and Winternitz, P., J. Physique **41**, 1391 (1980).
5. Abegg, R., *et al.*, Phys. Rev. Lett. **56**, 2571 (1986); Phys. Rev. D **39**, 2464 (1989).
6. Knutson, L.D., *et al.*, Phys. Rev. Lett. **66**, 1410 (1991); Vigdor, S.E., *et al.*, Phys. Rev. C **46**, 410 (1992); Vigdor, S.E., private communication.
7. Williams, A.G., Thomas, A.W. and Miller, G.A., Phys. Rev C **34**, 756 (1987); Ge, L. and Svenne, J.P., Phys. Rev. C **33**, 417 (1986); **34**, 756(E) (1986); Holzenkamp, B.H., Holinde, K. and Thomas, A.W., Phys. Lett B **195**, 121 (1987); Iqbal, M.J. and Niskanen, J.A., Phys. Rev. C **38**, 838 (1988) and private communication.
8. Niskanen, J.A., Phys. Rev. C **45**, 2648 (1992).
9. Niskanen, J.A. and Vigdor, S.E., Phys. Rev. C **45**, 3021 (1992).
10. Abegg, R., *et al.*, Nucl. Instrum. Methods A **234**, 11 (1985); **234**, 20 (1985); **254**, 469 (1987).
11. Abegg, R., *et al.*, Nucl. Instrum. Methods A **306**, 432 (1991).